Platelet activation attracts a subpopulation of effector monocytes to sites of *Leishmania major* infection

Ricardo Goncalves,[1] Xia Zhang,[1] Heather Cohen,[1] Alain Debrabant,[2] and David M. Mosser[1]

[1]Department of Cell Biology and Molecular Genetics and the Maryland Pathogen Research Institute, University of Maryland, College Park, MD 20782
[2]Center for Biologics Evaluation and Research, U.S. Food and Drug Administration, Bethesda, MD 20892

***Leishmania* species trigger a brisk inflammatory response and efficiently induce cell-mediated immunity. We examined the mechanisms whereby leukocytes were recruited into lesions after *Leishmania major* infection of mice. We found that a subpopulation of effector monocytes expressing the granulocyte marker GR1 (Ly6C) is rapidly recruited into lesions, and these monocytes efficiently kill *L. major* parasites. The recruitment of this subpopulation of monocytes depends on the chemokine receptor CCR2 and the activation of platelets. Activated platelets secrete platelet-derived growth factor, which induces the rapid release of CCL2 from leukocytes and mesenchymal cells. This work points to a new role for platelets in host defense involving the selective recruitment of a subpopulation of effector monocytes from the blood to efficiently kill this intracellular parasite.**

CORRESPONDENCE
David M. Mosser:
dmosser@umd.edu

Abbreviations used: CCR, CC-chemokine receptor; *Leishmania* spp., *Leishmania* species; MEF, mouse embryo fibroblast; PDGF, platelet-derived growth factor; TLR, Toll-like receptor.

Leishmania spp. are protozoan parasites that are responsible for a spectrum of diseases in the human host. The promastigote form of the parasite is transmitted into the skin of a mammalian host when an infected sandfly takes a blood meal. Promastigotes are rapidly taken up by professional phagocytic cells, and transform into the intracellular amastigote form. Parasites reside and replicate within macrophage phagolysosomes impervious to the low pH and acid hydrolases of this environment. Although virtually all phagocytic cells are capable of parasite phagocytosis, the macrophage appears to be the primary, if not exclusive, site for parasite replication. Successful host defense against this intracellular parasite involves the generation of antigen-specific T cells producing IFN-γ (Afonso and Scott, 1993). This results in the generation of classically activated macrophages, which are defined by their ability to kill this and other intracellular pathogens (Mosser and Edwards 2008; Yang et al., 2010).

Tissue macrophages can arise from one of two major sources. During steady state, resident tissue macrophages homeostatically arise from local tissue-resident progenitor stem cells, which repopulate mature tissue macrophages. During inflammation, however, monocytes from the blood represent the major source of macrophages. Monocytes rapidly exit the blood and transform into macrophages. In most localized inflammatory events involving leukocyte migration from the blood, neutrophils are the first cells to arrive, followed by monocytes, which replace the short-lived neutrophils and persist in tissue as macrophages until the inflammation subsides. There are two major subpopulations of monocytes, based on their morphology and physiology (Geissmann et al., 2003; Strauss-Ayali et al., 2007). These two monocyte populations can be identified by differential surface marker expression. In the mouse, the two major monocyte subpopulations are roughly equally represented in the blood. One of the populations expresses the granulocyte marker called GR1, which in monocytes and macrophages is now more commonly referred to as Ly6C. This subpopulation also expresses relatively high levels of the CC-chemokine receptor 2 (CCR2), but

R. Goncalves's present address is Dept. of Biological Science, Federal University of Ouro Preto, Ouro Preto, MG, Brazil.

The Rockefeller University Press $30.00
J. Exp. Med. Vol. 208 No. 6 1253-1265
www.jem.org/cgi/doi/10.1084/jem.20101751

moderate to low levels of the fractalkine receptor (CX3CR1; Palframan et al., 2001; Geissmann et al., 2003; Tsou et al., 2007; Auffray et al., 2009). The other monocyte subpopulation lacks the granulocyte marker (GR1) and CCR2, but expresses high levels of the fractalkine receptor (Palframan et al., 2001; Tsou et al., 2007). Jung et al. (2000) developed a mouse strain in which CX3CR1 was replaced with GFP, to allow the identification of the two major monocyte subpopulations. The $GR1^-$ cells, which express high levels of the fractalkine receptor, are GFP^{Bright}, whereas the $GR1^+$ cells, which express low levels of fractalkine receptor, are GFP^{Dull}. We used these and other mice to examine the kinetics of monocyte recruitment in response to *L. major* infection.

The recruitment of leukocytes to the site of *Leishmania* spp. infections has, until recently, been a relatively understudied area. There is ample historical evidence that mononuclear phagocytes are recruited to the site of infection, where they harbor intracellular parasites (Conrad et al., 2007; León et al., 2007; Villadangos 2007; Ng et al., 2008). Recent studies indicate that neutrophils are also rapidly recruited to the site of *Leishmania* infections (Peters et al., 2008). This efficient recruitment of leukocytes by *Leishmania* spp. is in stark contrast to the inability of this parasite to directly activate innate immune responses. These eukaryotic parasites fail to express many of the molecular patterns expressed on prokaryotes that efficiently activate Toll-like receptors (TLRs). Consequently, in vitro these organisms enter macrophages via a quiescent mechanism that fails to result in NF-κB activation and elicits negligible cytokine production (unpublished data). This silent mechanism of entry into phagocytes in vitro is not consistent with the inflammatory nature of many leishmanial lesions. Therefore, we set out to understand how these parasites were able to rapidly recruit leukocytes from the blood to the site of infection.

Platelets have long been appreciated to play an important role in hemostasis by virtue of their ability to become activated in response to damage to the vascular endothelium. Activated platelets exude pseudopods, assume a stellate shape, and self-aggregate to form platelet plugs. These platelet plugs can contribute to cardiovascular diseases because of thrombus formation after atherosclerotic plaque rupture. After binding to activated endothelium, activated platelets have been shown to promote the recruitment of monocytes, which play an important role in atherogenesis by differentiating into macrophages and causing the local inflammation (van Gils et al., 2009; Semple and Freedman, 2010). A role for platelets during inflammation and immune responses has been recently described (von Hundelshausen and Weber, 2007). Platelets are rapidly deployed to sites of infection where they can modulate immune/inflammatory processes by secreting cytokines, chemokines, and other inflammatory mediators (Smyth et al., 2009; Semple and Freedman 2010; Yeaman, 2010). A role for platelets during bacterial (Yeaman, 2010) and parasitic (van der Heyde et al., 2005) infections has recently been described. Platelets express TLRs that can bind to bacterial products and signal mediator secretion (Zhang et al., 2009; Beaulieu and Freedman, 2010), and platelets can cleave extracellular matrix components to produce inflammatory cleavage products (de la Motte et al., 2009). One of the major secretory products from the α-granules of activated platelets is platelet-derived growth factor (PDGF). PDGF has growth-promoting activity (Alberta et al., 1999; Andrae et al., 2008), but it is also a potent inducer of the chemotactic factor CCL2 (MCP-1) from a variety of immune and nonimmune cells (Alberta et al., 1999).

In this work, we examined the migration of monocyte subsets in response to *L. major* infection. We demonstrate that a subset of monocytes expressing high levels of CCR2 and the granulocyte marker GR1 are rapidly recruited to sites of *L. major* infection where they efficiently kill *L. major* parasites. Here, we examine the mechanism of monocyte recruitment, and the cells and factors that are involved in this process.

RESULTS

The kinetics of monocyte recruitment

We examined monocyte recruitment into *L. major* lesions using mice originally developed by Jung and Littman in which the fractalkine receptor (CX3CR1) was replaced by GFP (Jung et al., 2000). These mice were crossed to C57BL/6 mice to develop mice that were heterozygous for GFP, and therefore expressed a functional CX3CR1. Fig. 1 A shows a low magnification fluorescence photomicrograph of the two populations of blood monocytes from these mice. There are clearly two populations of cells that can be separated on the basis of fluorescence intensity. The GFP^{BRIGHT} cells express low or undetectable levels of the granulocyte marker GR1, whereas the GFP^{LOW} cells express high levels of GR1 (Fig. 1 B). In uninfected mice, these two monocyte populations are roughly equally represented in the blood (Fig. 1 B; Geissmann et al., 2003).

Because $CX3CR1^{GFP}$ mice express GFP only in monocytes and some undefined subsets of NK cells (Jung et al., 2000), we performed a flow cytometry analysis using these mice to examine monocyte subpopulations in the footpads during infection. The cells were isolated from the footpads and stained for F4/80 and CD11b to avoid NK cell contamination during the analysis. As expected, we found low numbers of monocytes in the footpads of uninfected mice (Fig. 1 C, top). At 24 h after infection with *L. major*, however, there was a dramatic increase in the number of GFP^{LOW} monocytes in the footpads of infected mice. The percentage increased from 5.33 to 16.4% within the first 24 h of infection (Fig. 1 C, bottom). These rapidly migrating monocytes express the granulocyte marker GR1 (Fig. 1 C, right). We performed a kinetic analysis of monocyte recruitment into leishmanial lesions using the GFP mice crossed onto a $RAG^{-/-}$ background where 50% of the leukocytes in the blood are monocytes. By as early as 30 min and 1 h after infection, we began to observe $GR1^+$ monocyte entry into infected footpads (Fig. 1 D). By 2 h, there was a pronounced accumulation of these monocytes at the site of infection. The rapid migration of these monocytes into lesions preceded even that

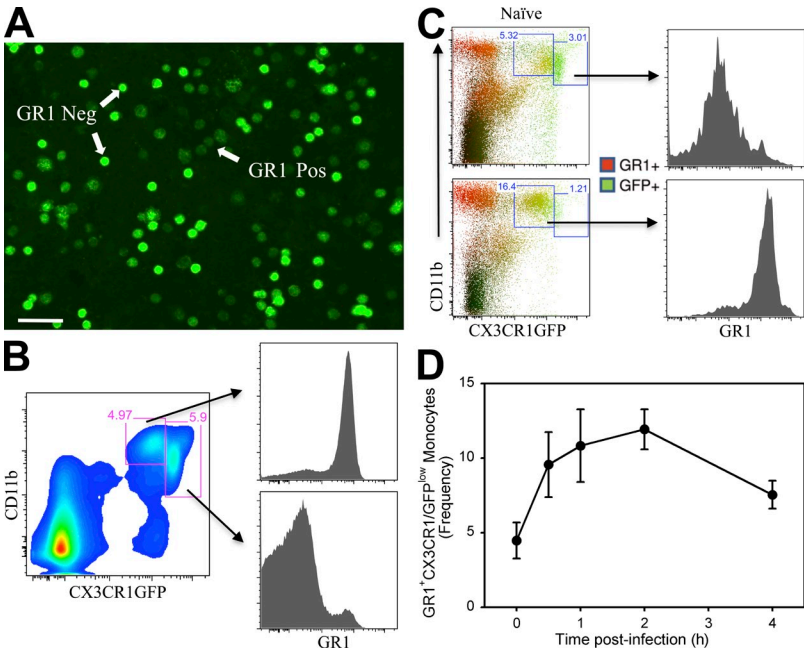

Figure 1. The identification of inflammatory monocytes during *L. major* infection. (A) Fluorescent microscopy of PBMC from uninfected CX3CR1$^{GFP/+}$ RAG2$^{-/-}$ transgenic mice showing GFP^{High} (GR1^{-}) and GFP^{Low} (GR1^{+}) cells. (B) Flow cytometry analysis of blood monocytes (PBMC) from CX3CR1$^{GFP/+}$ mice showing that GR1^{+} monocytes (top right histogram) are derived from the GFP ^{low} population of blood monocytes, whereas GR1^{-} monocytes (bottom right histogram) are derived from the GFP^{High} population of monocytes. (C) Flow cytometry analyses of cells from the footpads of CX3CR1$^{GFP/+}$ mice before (top) and 24 h after (bottom) infection with 2 × 10^{6} *L. major*. Cells were gated based on FSC x SSC profile eliminating dead cells and debris, using the F4/80^{+} antibody. The numbers represent the frequency of gated cells. This plot is representative of at least three experiments using five mice per group. (D) The frequency of GR1^{+} monocytes in infected footpads at the designated times after infection. The numbers represent the mean of the frequency of gated cells taken from three experiments using three mice per group. Bar, 50 µm.

of PMNs, which were found in low numbers in lesions at 30 min and 1 h, but began to show a substantial accumulation by 2 h (unpublished data). The decreased frequency at 4 h (Fig. 1 D) was caused by the accumulation of neutrophils. Thus, a population of monocytes expressing the granulocyte marker GR1 rapidly exits the blood and enters into lesions in response to *L. major* infection.

A similar kinetic analysis was performed after *L. major* infection in the peritoneum of mice, because this anatomical location allows for the convenient collection of large numbers of monocytes for subsequent analysis. We could readily identify three leukocyte populations in the peritoneum, based on forward and side scatter and CD11b and F4/80 expression. The identity of each population was confirmed by morphology after fluorescence-activated cell sorting. The F4/80-high cells were resident peritoneal macrophages, the F4/80-intermediate cells were newly migrated monocytes, and the F4/80-low/absent cells were neutrophils (Fig. 2 C).

We observed a rapid migration of monocytes into the peritoneum in response to intraperitoneal *L. major* infection. Monocytes began to accumulate within 30 min of *L. major* infection in both BALB/c and C57BL/6 mice (Fig. 2 A). Over the first hour, the percentage of monocytes, designated by the F4/80 intermediate quadrant, increased from 5.08 to 20.8% in the BALB/c mouse and from 8.03 to 17% in the C57BL/6 mouse. This rapid migration of monocytes into the peritoneum preceded that of neutrophils, which did not exhibit substantial accumulation until 2 h after infection in the BALB/c mouse and 1 h in the C57BL/6 mouse (Fig. 2 A). The majority of rapidly migrating monocytes in response to *L. major* infection expressed the GR1 marker (Fig. 2 B). To demonstrate that our gating was able to correctly distinguish between the various leukocyte populations, cytospin preparations of sorted F4/80 intermediate cells were examined. They showed the typical mononuclear cell morphology of monocytes, and there were virtually no polymorphonuclear cells in this F4/80 intermediate population. At this early time after infection, several intact and partially degraded intracellular *L. major* parasites could be observed within monocytes at the light microscopic level (Fig. 2 C, arrows). The F4/80$^{Low/Neg}$ cells had the typical polymorphonuclear morphology of neutrophils. To our surprise, we were not able to detect any intracellular parasites within these neutrophils.

Monocyte killing of *L. major*

We took advantage of red fluorescent protein (RFP)-*L. major* parasites, which were developed by one of the authors (Kimblin et al., 2008), to quantify parasite numbers in peritoneal monocytes in situ shortly after infection. By 1 h after infection, there was a large increase in the number of RFP-positive (infected) monocytes in the peritoneum (Fig. 3 A, middle), relative to uninfected controls (left). The majority of these infected cells stained positively for GR1. This is also shown in the histogram in Fig. 3 B, where at 1 h, the majority of GR1^{+} monocytes are infected with RFP-*L. major* (top). By as early as 4 h after infection, however, we detected very few intact RFP-*L. major* in these monocytes. In Fig. 3 A, the double-positive population decreased from 41% (middle) to 0.32% (right). This is confirmed in the histogram in Fig. 3 B (bottom), where at 1 h the majority of parasites are located in the GR1^{+} population of monocytes. At 4 h, only a small shoulder of RFP-positive monocytes expressing GR1 was visible. The GR1^{-} monocytes, in contrast, show a lower percentage of infected cells at 1 h, designated by the small shoulder of RFP-positive cells (Fig. 3 B, top right profile), and this low level of infection remains essentially unchanged

after 4 h (Fig. 3 B, bottom right profile). The extent of RFP-*L. major* associated with monocyte subpopulations from three pooled experiments are shown in Fig. 3 C. In all cases, the GR1$^+$ monocytes isolated from the peritoneum at 1 h after infection contained the majority of RFP parasites, and these parasites were rapidly cleared by 4 h. Thus, GR1$^+$ monocytes rapidly enter the peritoneum and associate with *L. major* parasites, and within 4 h the majority of these organisms are degraded and no longer visible within these cells.

To directly address parasite killing by monocytes, in vitro infections were undertaken, using purified monocyte subpopulations from CX3CR1$^{GFP/+}$RAG2$^{-/-}$ mice obtained by fluorescence-activated cell sorting. Metacyclic *L. major* promastigotes were added to the two populations of monocytes and the number of RFP-*L. major* per monocyte was determined at 60 min and at 3 h after infection. The GR1$^+$ subpopulation of monocytes bound avidly to *L. major*, and at 60 min the majority of monocytes had at least 1 parasite attached to it and many of these monocytes had several parasites associated with them (Fig. 4 A). These monocytes appeared to rapidly kill *L. major* parasites, because by as early as 3 h after incubation, there were substantially fewer intact parasites associated with the GR1$^+$ subpopulation of monocytes. The majority of the monocytes no longer had parasites associated with them and only a small percentage of the

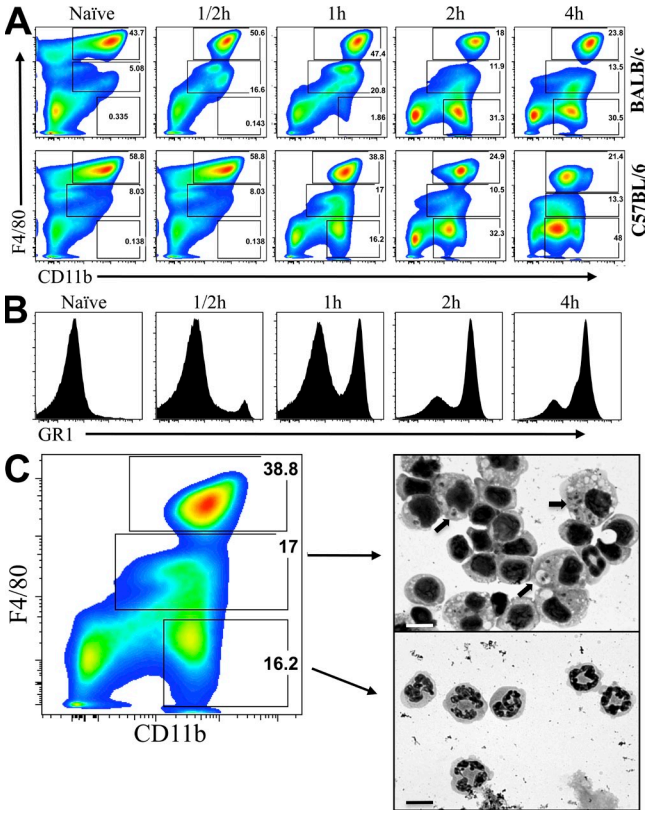

Figure 2. Monocyte migration into the peritoneum in response to infection with *L. major* promastigotes. (A) Flow cytometry analysis showing the kinetics of leukocyte infiltration into the peritoneum after infection with 2 × 10^6 *L. major* parasites. Three distinct populations of cells, identified by gating on CD11b and F4/80 levels, are designated by boxed areas. (B) Histograms showing GR1 expression on the F4/80^{Int}CD11b$^+$ monocytes between 30 min and 4 h after peritoneal infection with 2 × 10^6 *L. major*. (C) Cytospin analysis of F4/80^{Int} monocytes and F4/80^{Neg} neutrophils after 1 h of peritoneal infection of C57BL/6 mice. Cells were gated based on FSC x SSC profile, eliminating dead cells and debris. Arrows point to *L. major* parasites inside cells. The numbers represent the frequency of gated cells from one experiment, and are representative of at least 4 experiments using a total of 40 mice. Bars, 10 µm.

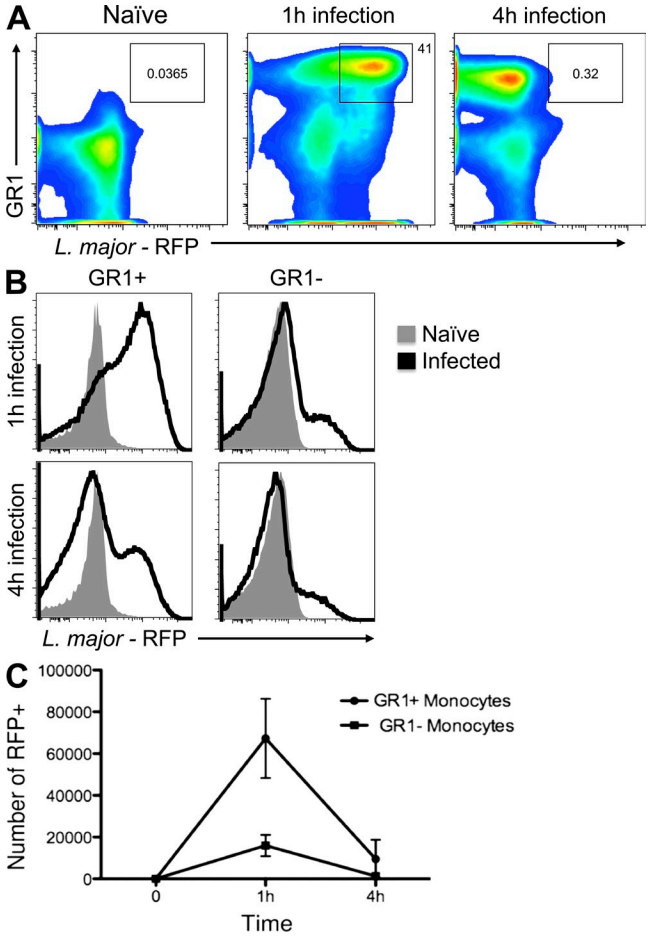

Figure 3. The rapid killing of *L. major* parasites by GR1$^+$ monocytes. (A) Flow cytometry profiles of monocytes gated on F4/80$^+$CD11b$^+$GR1$^+$ monocytes at 1 and 3 h after infection with RFP-*L. major*. Uninfected (naive) cells show no RFP staining (left profile). (B) Histograms showing GR1$^+$ monocytes (left) or GR1$^-$ monocytes (right) infected with RFP-*L. major* after 1 h (top) or 4 h (bottom) with 2 × 10^6 RFP-*L. major*. (C) The number of infected (RFP-positive) F4/80$^+$CD11b$^+$ GR1$^+$ monocytes (circles) and GR1$^-$ monocytes (squares) after peritoneal infection with 2 × 10^6 *L. major* parasites. Cells were gated based on FSC x SSC profiles to eliminate dead cells and then separated using antibodies to F4/80 and CD11b. The number showed in dot plots represent the frequency of gated cells from one experiment and are representative of 3 independent experiments using a total of 18 mice. The numbers on the y axis represent the mean of the absolute numbers of infected monocytes, and the error bars are the SD from three independent experiments.

monocytes had more than 1 intact parasite associated with them (Fig. 4 A).

The number of *L. major* parasites associated with monocytes at 1 and 3 h was quantitated from three independent experiments (Fig. 4 B). After 1 h, there was an average of 1.6 parasites associated with each GR1$^+$ monocyte, and this number declined by approximately half by as little as 3 h. Parasite association with the GR1$^-$ population of monocytes was also examined and compared with the GR1$^+$ population. The GR1$^-$ monocytes bound fewer parasites at 1 h than did the GR1$^+$ cells, and the number of parasites associated with these cells at 3 h was slightly increased relative to the number bound at 1 h (Fig. 4, A and B).

We also undertook long-term in vitro infection studies, in which metacyclic promastigotes were added to monocytes and incubated unwashed for 3 d. At this time, parasite viability was quantitated by limiting dilution. The GR1$^+$ monocytes efficiently killed metacyclic *L. major* promastigotes, and by 3 d there were no viable parasites in the cultures (Fig. 4 C). In contrast, the GR1$^-$ population was less efficient at killing *L. major* parasites, and there remained a substantial number of viable parasites in these cultures (Fig. 4 C).

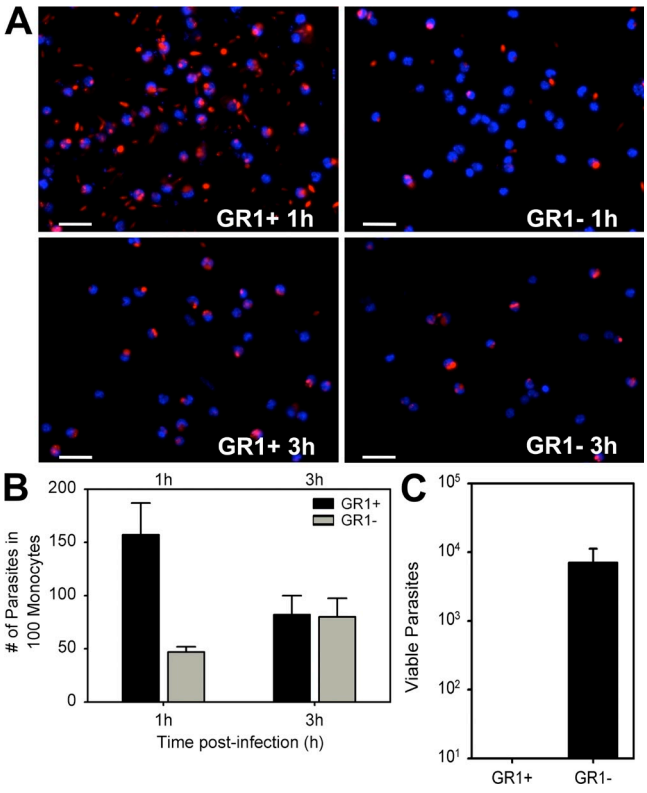

Figure 4. The in vitro killing of *L. major* by GR1$^+$ monocytes from wild-type mice. (A) GR1$^+$ (left) and GR1$^-$ (right) monocytes were sorted from CX3CR1$^{GFP/+}$ RAG2$^{-/-}$ mice by GFP expression and incubated with 10:1 ratio of metacyclic RFP-*L. major* in vitro. Fluorescence photomicrographs of gently washed monolayers were taken after 1 h (top) or 3 h (bottom). (B) The total mean number of *L. major* parasites ($n = 3$) associated with GR1$^+$ or GR1$^-$ monocytes after 1 or 3 h in vitro infection. (C) GR1$^+$ and GR1$^-$ monocytes were sorted based on CX3CR1^{GFP} expression and incubated with 5:1 ratio of *L. major* to monocytes in vitro. The cells were kept in culture for 3 d at 37°C without washing. After 3 d, parasite numbers were calculated by serial dilution assays. Data represent the mean ± SE of 3 independent experiments using a total of 40 mice. Bars, 50 µm.

The monocyte respiratory burst

Despite the fact that we added an excess of parasites to the GR1$^+$ monocyte cultures (a 5:1 ratio of parasites to monocytes), all of the parasites in the culture were killed within 3 d. We therefore visually examined the parasites at earlier times after infection to look for early evidence of parasite killing. Incubation of parasites with GR1$^+$ monocytes resulted in a rapid alteration in parasite morphology (Fig. 5 A) and a dramatic decrease in parasite mobility (Fig. 5, C and D and Video 1). Normal metacyclic promastigotes exhibit a slender

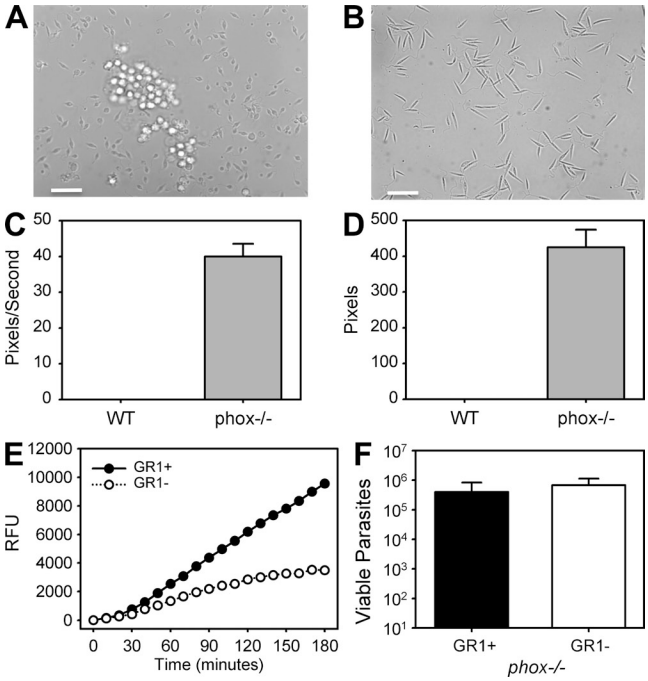

Figure 5. The in vitro killing of *L. major* parasites by GR1$^+$ monocytes from wild-type and from phox$^{-/-}$ mice. (A) Phase-contrast microscopy taken on an inverted photomicroscope of sorted wild-type GR1$^+$ monocytes showing altered morphology of unfixed metacyclic *L. major* promastigotes when cultivated with (A) or without (B) GR1$^+$ monocytes for 1 h. (C and D) GR1$^+$ monocytes were isolated from wild-type (WT) or gp91 phox$^{-/-}$ mice and sorted by F4/80 and GR1 expression. Monocytes were incubated with 5:1 ratio of *L. major* to monocytes in vitro. At 3 h the movement of extracellular promastigotes was determined using ImageJ software to calculate the mean distance (C) and velocity (D) from 20 selected parasites per culture. At least 30 mice were used in 2 independent experiments. (E) The in vitro production of ROS. The kinetics of ROS production from sorted GR1$^+$ and GR1$^-$ infected monocytes in the presence of H_2DCFDA measured by fluorometry. Data are from three independent experiments. (F) Monocytes from WT or phox$^{-/-}$ mice were cultivated with *L. major* for 3 d without washing, at which time parasite viability was determined by limiting dilution assay. Data are the mean ± SEM from three independent experiments involving at least 20 mice. Bars, 50 µm.

morphology (Fig. 5 B) and move very rapidly in liquid culture. Even the extracellular parasites that were not attached to GR1$^+$ monocytes stopped their movement and took on a rounded morphology that is frequently observed in dying parasites. Parasites associated with the GR1$^-$ subpopulation of monocytes, in contrast, did not exhibit this alteration in morphology and their movement did not slow (Video 2).

To examine the mechanism of killing, we measured the monocyte respiratory burst after the addition of metacyclic *L. major* promastigotes to monocytes in vitro. Superoxide production by each subpopulation of monocytes was measured by chemiluminescence of H_2DCFDA. The GR1$^+$ subpopulation of monocytes rapidly produced detectable amounts of superoxide in response to *L. major* infection. By 30 min, the signal was above background and by 60 min it was substantially higher than that produced by the GR1$^-$ subpopulation of monocytes (Fig. 5 E). These cells continued to produce high levels of superoxide for the 180-min observation period (Fig. 5 E). The GR1$^-$ subpopulation also produced measurable amounts of superoxide in response to *L. major* infection. However the levels of superoxide production by these cells were substantially lower than the GR1$^+$ subpopulation (Fig. 5 E). At the single-cell level, superoxide production from infected monocytes was visualized by H_2DCFDA staining (Fig. S1). By 60 min after the addition of metacyclic promastigotes, many of the monocytes had promastigotes that were peripherally attached before internalization. Monocytes with peripherally attached parasites made substantial amounts of superoxide and stained brightly with H_2DCFDA (Fig. S1). Therefore, ample superoxide production by these monocytes occurred even before the parasites were internalized.

To further analyze the role of the monocyte respiratory burst in *L. major* killing, we performed in vitro killing assays using monocytes from gp91(phox)$^{-/-}$ monocytes. gp91(phox) is an essential component of the membrane-bound oxidase of phagocytes that generates reactive oxygen species. Neither GR1$^+$ nor GR1$^-$ monocytes from gp91 (phox) knockout mice were able to efficiently kill *L. major* parasites over the 3-d culture period (Fig. 5 F). Although there were slightly fewer viable parasites associated with the GR1$^+$ monocytes, both subpopulations of cells supported large numbers of viable *L. major* parasites, as determined by limiting dilution assay (Fig. 5 F). Furthermore, the dramatic alterations in parasite morphology and mobility that occurred with wild-type GR1$^+$ monocytes was not observed in parasites cultivated with GR1$^+$ monocytes deficient in the respiratory burst (Fig. 5, C and D). These parasites retained their morphology and moved rapidly in the culture medium (Video 3; for tracking of parasite movement, see Video 4).

Monocyte mobilization in response to platelet activation

We examined the mechanism of monocyte migration in response to *L. major* infection. Previous work of others demonstrated that the GR1$^+$ monocyte subpopulation expresses high levels of CCR2 (Palframan et al., 2001; Geissmann et al., 2003). Therefore, we examined monocyte migration into the peritoneum in normal C57BL/6 mice

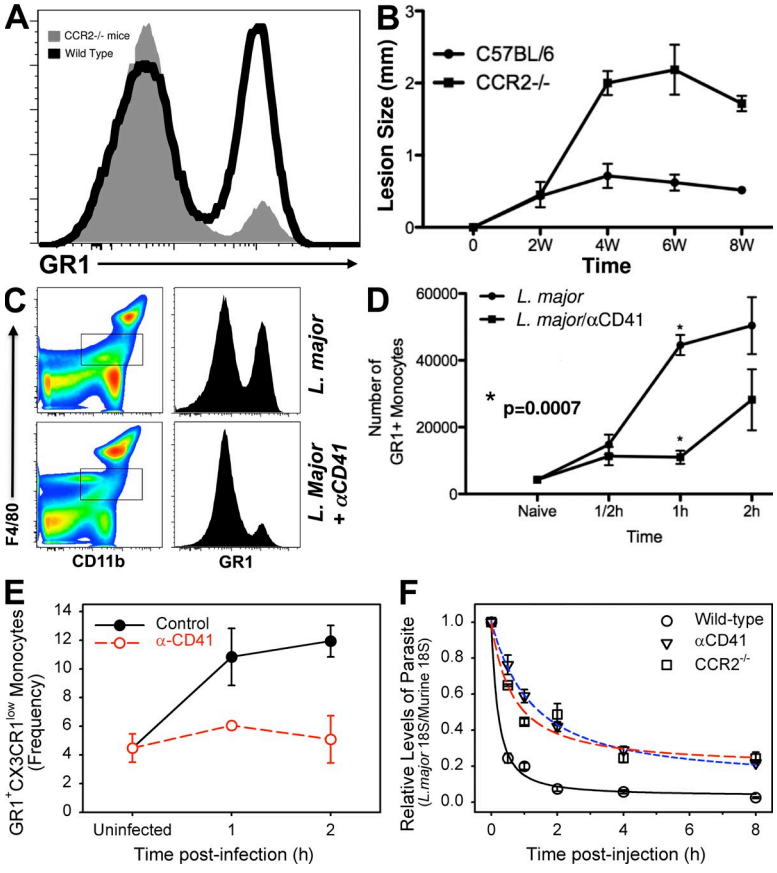

Figure 6. The role of CCR2 in the recruitment of GR1$^+$ monocytes. (A) Flow cytometry histograms comparing the recruitment of F4/80$^+$CD11b$^+$GR1$^+$ monocytes in CCR2$^{-/-}$ (gray profile) or wild-type (black profile) mice after 2-h infection with 2 × 10^6 *L major* parasites. (B) Lesion size in CCR2$^{-/-}$ (squares) and wild-type C57BL/6 (circles) mice after infection with 2 × 10^6 *L major* parasites. (C) Flow cytometry profiles showing the recruitment of F4/80 intermediate, GR1$^+$ monocytes into the peritoneum of mice after infection with 2 × 10^6 *L major* promastigotes, before (top right) or after (bottom right) treatment with αCD41 antibody to deplete platelets. (D) The number of GR1$^+$ monocytes in the peritoneum after infection with 2 × 10^6 *L major* promastigotes in untreated mice (circles) or mice treated with αCD41 antibody to deplete platelets (squares). (E) The mean frequency of GR1$^+$ monocytes recruited to footpads after *L major* infection with or without prior depletion of platelets using αCD41 antibody. At least three mice per group were used in three independent experiments. (F) In vivo killing of *L. major* parasites. C57BL/6 mice were depleted of platelets with α-CD41 or not and CCR2$^{-/-}$ mice were infected with 10^6 metacyclic *L major* promastigotes in the hind footpad. At different times, the footpads were collected and RT-PCR was performed to measure parasite levels, as described in experimental procedures. Data are representative of two independent experiments using at least three mice per group.

compared with mice lacking CCR2. Mice lacking CCR2 showed a profound defect in the rapid migration of the GR1$^+$ subpopulation of monocytes into the peritoneum in response to *L. major* infection (Fig. 6 A). The lack of "effector" monocyte migration in response to the parasite suggested that these mice should be more susceptible to *L. major* infection. That is what had previously been reported (Sato et al., 2000) and what we observe in Fig. 6 B. Mice deficient in the migration of this population of monocytes developed larger lesions than wild-type mice (Fig. 6 B). Because both of these mice are on the genetically resistant (C57BL/6) background, even the CCR2-deficient mice were eventually able to mount appropriate adaptive immune responses, which began to promote the clearance of the parasite (Fig. 6 B, 8 wk). Thus, CCR2 is an important mechanism in the recruitment of effector monocytes to limit early infections.

In measuring the migration of monocyte subsets into the peritoneum, we noticed the clustering of platelets around *L. major*. Because activated platelets can represent an important source of chemoattractants and mediators, we examined monocyte recruitment in C57BL/6 mice infected with *L. major* in the presence or absence of platelets. Mice were administered antibody to CD41 to deplete platelets. This treatment results in a transient depletion of 75–90% of platelets (Fig. S2). Platelet depletion with αCD41 resulted in a dramatic decrease in GR1$^+$ monocyte recruitment into the peritoneum in response to *L. major* infection (Fig. 6 C). After only 1 h of infection of normal mice with *L. major*, the number of GR1$^+$ monocytes in the peritoneum increased from baseline to >42,000 (Fig. 6 D), whereas prior depletion of platelets resulted in an accumulation of <10,000 monocytes over that time. In mice depleted of platelets, monocyte recruitment into the peritoneum does not approach wild-type levels for >2 h (Fig. 6 D). We performed a similar analysis to examine the recruitment of GR1$^+$ monocytes into the footpads of infected mice in the presence or absence of platelets (Fig. S3). Prior depletion of platelets with antibody to CD41 virtually eliminated the migration of GR1$^+$ monocytes into the footpads of infected mice in response to *L. major* infection (Fig. 6 E).

We examined the killing of *L. major* in the footpads of infected mice that were administered antiplatelet antibodies. In untreated wild-type mice, the number of parasites in the foot rapidly declined over the first 2 h. There was an 80% reduction in parasite DNA by 1 h and a 95% reduction by 2 h (Fig. 6 F). In mice administered antibodies to platelets, however, the killing did not occur as rapidly, and by 2 h after infection the amount of parasite DNA was reduced by <50% (Fig. 6 F). These differences in parasite killing persisted for the first 8 h. The delay in parasite killing in platelet-depleted mice is comparable to the delay in parasite killing that occurs in mice lacking CCR2 (Fig. 6 F). Thus, in the two groups of mice that are deficient in effector monocyte migration, there is a delay in parasite killing at the site of infection that is consistent with a role for these monocytes in early parasite killing at the site of infection.

Platelet activation by parasites depends on complement activation

To determine the mechanism whereby *L. major* promastigotes activate platelets, we incubated *L. major* with platelets in the presence or absence of serum as a source of complement. We and many other groups have previously demonstrated that *Leishmania* spp. are efficient activators of complement (Mosser and Edelson 1987; Mosser et al., 1992). We used platelet aggregation as a well-established indicator of platelet activation. The co-incubation of platelets and *L. major* alone or in heat-inactivated serum had essentially no effect on platelets. The platelets remained round and did not associate with the parasites or each other (Video 5). However, the addition of nonimmune serum to platelets and *L. major* resulted in the rapid activation of platelets and the clustering of parasites and platelets together into large aggregates (Fig. 7, A and B). This activation of platelets did not occur in serum from mice deficient in the third component of complement, C3, indicating that the early components of complement activation were required for this effect (Fig. 7 B). C5-deficient serum fully supported platelet activation (Fig. 7 B). Platelet activation occurred very rapidly (Video 6), and by as early as 5 min aggregates of platelets and parasites could be visualized. By 10 min, platelets were in large clumps associated with multiple *L. major* parasites (Fig. 7 B and Video 6).

In addition to platelet aggregation, another well-established indicator of platelet activation is the expression of P-selectin (CD62P) on the surface of activated platelets. We measured CD62P expression on platelets by flow cytometry. After a 30-min incubation of *L. major* with platelets in the presence of nonimmune C5-deficient serum, a substantial percentage of platelets expressed CD62P on their surface and an increased expression of CD41 (Fig. 7 C). Thus, platelet activation is dependent on complement activation. To determine whether GR1$^+$ monocyte recruitment was dependent on the activation of complement, we examined the number of monocytes migrating into the peritoneal cavity of mice deficient in the third component of complement, C3, and compared this to complement-sufficient mice. Mice lacking opsonic complement attracted substantially fewer monocytes into the peritoneum in response to *L. major* infection, and of these monocytes a much smaller percentage of them were effector monocytes that express GR1$^+$ on their surface (Fig. 7 D). Therefore, *Leishmania* spp. activate platelets via the activation of complement to recruit effector monocytes.

Several groups have reported that platelet activation results in the release of PDGF (Yeaman 2010; Fox 2001). We measured the release of PDGF after the co-incubation of platelets with *L. major* promastigotes (Fig. 8 A). The isolation of platelets from normal mouse serum resulted in a small degree of PDGF release caused by the isolation procedure itself. However, the in vitro co-incubation of platelets with *L. major* and normal plasma resulted in a substantial increase in PDGF release (Fig. 8 A). PDGF is a potent inducer of CCL2 (MCP-1) release from several different cell types, including fibroblasts (Strieter et al., 1989), macrophages (Yoshimura et al., 1989),

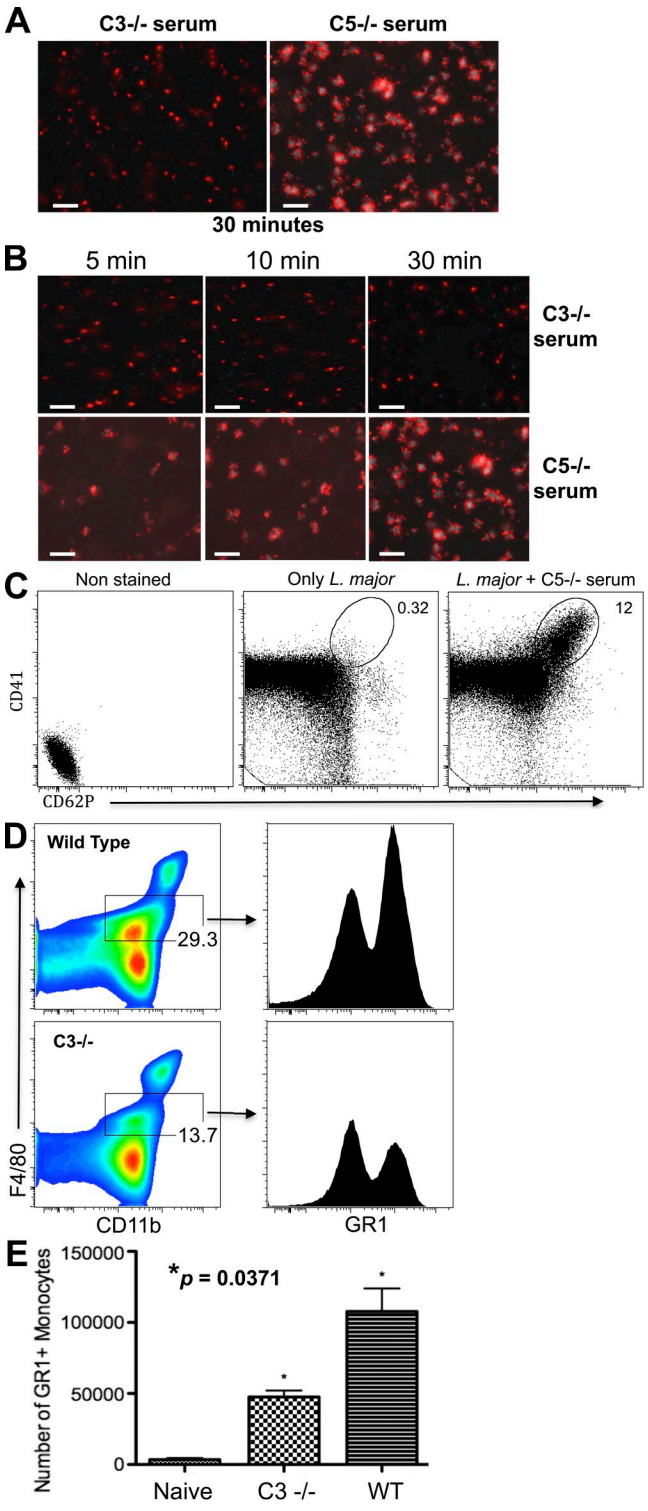

Figure 7. Platelet activation by *L. major* parasites. (A) Fluorescence photomicroscopy showing RFP-*L. major* parasites and CFP-labeled platelets that were incubated for 30 min in the presence of fresh nonimmune serum from $C3^{-/-}$ mice (left) or $C5^{-/-}$ mice (right). (B) 2×10^7 CFP-platelets were incubated with 10^6 parasites for 1–30 min in the presence of serum from mice lacking C3 ($C3^{-/-}$; top) or C5 ($C5^{-/-}$; bottom), and then observed by fluorescence microscopy. (C) CD62P expression on platelets activated by *L. major* and complement. Left profile, platelets alone with no antibody; middle profile, *L. major* promastigotes plus platelets but no serum, stained with αCD41; right profile, *L. major* plus complement and platelets, stained with αCD41. (D) Monocyte recruitment into the peritoneal cavity of wild-type C57BL/6 (top) or $C3^{-/-}$ (bottom) mice after 4 h of infection with 2×10^7 *L. major* parasites. The $CD11b^+$ $F4/80^{Int}$ population was analyzed for GR1 expression (right profiles). (E) The total number of $GR1^+$ monocytes migrating into the peritoneal cavity of wild-type or $C3^{-/-}$ mice after infection with *L. major*. The platelet activation experiments (A–C) were performed >5 times using at least 10 mice/experiment. The experiments using $C3^{-/-}$ mice (D and E) mice were performed twice using 12 mice.

and endothelial cells (Rollins et al., 1990). We measured the release of CCL2 (MCP-1) from mouse embryo fibroblasts (MEFs) after their incubation with *L. major*, platelets, and normal plasma. The combination of parasites, plasma, and platelets resulted in the release of substantial amounts of CCL2 (MCP-1) from MEFs (Fig. 8 B). This release was caused by the activation of platelets because in the absence of platelets *L. major* alone induced substantially less CCL2 (MCP-1) from MEFs (Fig. 8 B). Furthermore, in the presence of antibody to the PDGF receptor, CCL2 (MCP-1) production was substantially reduced (Fig. S4).

We next examined local PDGF and CCL2 (MCP-1) production at the site of infection in the footpads of mice infected with *L. major*. PDGF was rapidly produced in response to *L. major* infection (Fig. 8 C). PDGF production peaked by 20–30 min and began to decline thereafter. PDGF is a potent inducer of CCL2 (MCP-1) production. Therefore, we examined CCL2 (MCP-1) production at the site of infection. CCL2 (MCP-1) was also rapidly produced in the foot in response to *L. major* infection. CCL2 (MCP-1) levels peaked by 30 min and remained high for 60 min (Fig. 8 D). The depletion of platelets with antibody to CD41 resulted in the decreased production of both PDGF (Fig. 8 C) and CCL2/MCP-1 (Fig. 8 D) at the site of infection. Thus, platelet activation by *L. major* results in the production of PDGF by platelets, which induces the local release of CCL2 (MCP-1) to recruit a subpopulation of CCR2-positive monocytes into leishmanial lesions. These monocytes rapidly kill *L. major*.

DISCUSSION

This work describes the rapid mobilization of a monocyte subpopulation from the blood after infection with the intracellular protozoan parasite, *Leishmania major*. These monocytes efficiently kill these parasites. There were several unexpected observations that emerged from this work. The first pertained to the mechanism whereby effector monocytes were mobilized from the blood. *Leishmania* spp. are eukaryotic parasites that lack many of the pattern associated molecular patterns typically displayed on prokaryotes. Despite this apparent lack of TLR activation, these organisms efficiently recruit leukocytes into the sites of infection. We show that this recruitment occurs by a unique mechanism that involves the rapid activation of platelets. The phenomenon of *Leishmania* spp. parasites binding to cells in the blood was previously

termed "immune adherence" (Domínguez and Toraño 2001). This phenomenon is dependent on the activation of complement, and more than two decades ago, the activation of platelets by complement was shown to be mediated by platelet complement receptors (Fukuoka and Hugli 1988). Here, we demonstrate that complement activation by *Leishmania* spp. causes platelets to bind to *L. major* and release PDGF. Several investigators have previously demonstrated that PDGF is an efficient inducer of CCL2 (MCP-1) production from a variety of cells, including endothelial and fibroblastoid cells and smooth muscles (Yoshimura and Leonard 1990; Poon et al., 1996; Deshmane et al., 2009). We demonstrate that PDGF production from activated platelets induces the release of CCL2 to recruit effector monocytes to the site of infection by virtue of their expression of CCR2 (Palframan et al., 2001; Geissmann et al., 2003). Thus, this work points to an unexpectedly specific role for platelets in early host defense. The second unexpected aspect of this work was the speed with which these effector monocytes were dispatched to parasites. Dogma holds that PMNs are the first cells to enter inflammatory sites, but in this model a subpopulation of inflammatory monocytes accumulated even before PMNs were mobilized. Recent work has shown that large amounts of neutrophils are attracted to the site of *L. major* infection after the bite of an infected sandfly (Peters et al., 2008). In those studies, neutrophils failed to kill intracellular *L. major*. In light of these observations, we would propose that the parasites would be efficiently killed in the presence of effector monocytes, whereas those parasites that enter resident tissue macrophages or perhaps neutrophils may escape monocyte killing and establish infection. The rapid recruitment of $GR1^+$ monocytes in response to thioglycollate administration was previously reported by Henderson et al. (2003). They demonstrated that this population of monocytes was recruited into the peritoneum independently of neutrophils. Auffray et al. (2007), however, demonstrated that the $GR1^-$ monocyte subpopulation, which exhibits a patrolling behavior in the blood, could rapidly immigrate to the site of infection with *Listeria monocytogenes*. This migration preceded that of $GR1^+$ monocytes and neutrophils. In the present study, we describe the rapid migration of the $GR1^+$ subpopulation of monocytes in response to *L. major* infection, and we demonstrate that this migration is dependent on platelet activation and the elaboration of CCL2.

It has been appreciated for some time that monocytes could be separated into different subpopulations, based on their morphology and the expression of specific markers (Ziegler-Heitbrock et al., 1988; Passlick et al., 1989). It was not until the important work of Jung et al. (2000) that monocyte subpopulations could be marked with GFP, allowing them to be analyzed during homeostasis, inflammation, and infection. There appear to be a variety of distinct fates for these monocytes subsets after they leave the blood. Monocytes expressing the GR1 marker have been shown to differentiate into a population of dendritic cells that make large amounts of TNF (Serbina et al., 2003). They also appear to be capable of differentiating into macrophages with an alternatively activated phenotype (Auffray et al., 2007) or even into microglia (Getts et al., 2008). Recent studies by other groups have begun to reveal an important role for these "effector" monocytes during infectious diseases, such as malaria (Sponaas et al., 2009). The production of type I interferon by these cells in response to viral infections has recently been reported (Barbalat et al., 2009). Consistent with our observations, Dunay et al. (2008) demonstrated that these cells are important effector cells during *Toxoplasma gondii* infections. These cells have recently been shown to control the growth of YopM-negative *Yersinia pestis* (Ye et al., 2009). The direct demonstration that these

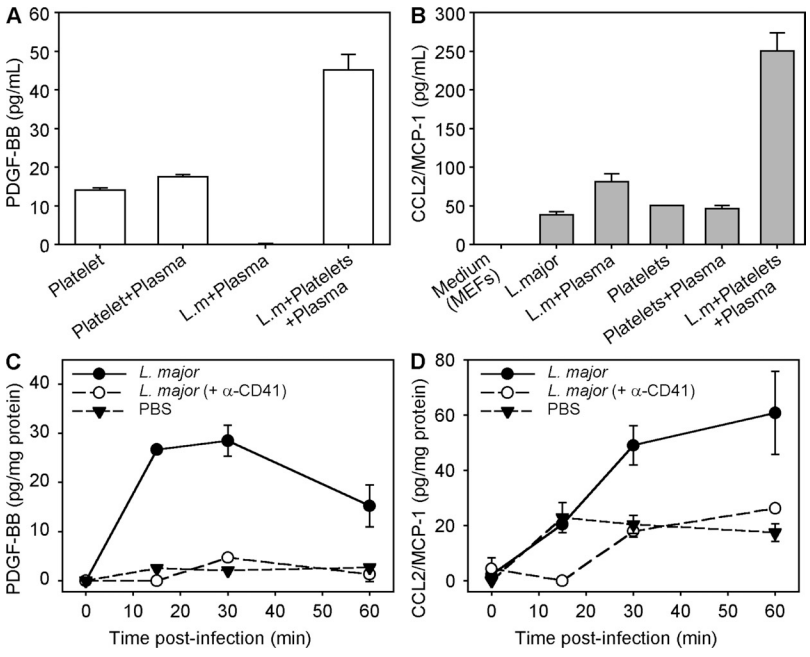

Figure 8. Chemotactic activity associated with the activation of platelets. (A) Platelets were isolated from normal mice and incubated with *L. major* promastigotes in the presence or absence of plasma as a source of complement. The release of PDGF from activated platelets after 30-min incubation was measured by ELISA. (B) CCL2 (MCP-1) production by MEF exposed to activated platelets was measured by ELISA. MEFs were incubated in culture medium alone, medium containing *L. major*, or medium containing *L. major* and fresh plasma for 30 min. (C and D) Mice were injected in the footpad with 25 µl saline alone (filled triangles) or saline containing 2×10^6 *L. major* parasites (filled circles). 24 h before infection some mice received 2 µg anti-CD41 antibody i.p. to deplete platelets (open circles). The production of PDGF (C) or CCL2/MCP-1 (D) was measured by ELISA and normalized to the total protein. Data represent the mean ± SE of the mean, from 3 independent experiments using a total of 15 mice. Data on platelet depletion was performed on five mice.

monocytes are able to kill parasites had not been made, and the mechanisms whereby these cells are recruited from the blood into tissue had not been previously explored.

The present work on monocyte killing of *L. major* promastigotes inadvertently extends observations made by us ~20 yr ago that complement activation was important for the efficient phagocytosis of *Leishmania* spp. (Mosser et al., 1992). We now show another mechanism whereby complement improves *L. major* clearance in nonimmune hosts. The activation of complement by *Leishmania* spp. results in the activation of platelets to recruit a monocyte subpopulation that can rapidly kill *L. major*. We examined the mechanisms responsible for the rapid killing of *L. major* parasites by the $GR1^+$ monocytes. These effector monocytes produce high levels of superoxide when encountering *L. major* parasites, consistent with this being a mechanism that contributes to parasite killing. Monocytes that were unable to produce a respiratory burst because of the lack of gp91(phox) were unable to kill *L. major* parasites. These monocytes also failed to induce the profound changes in parasite morphology and mobility that we observed. These data argue that superoxide is necessary for parasite killing, but they do not address whether oxygen radicals are sufficient to mediate *L. major* parasite killing. In several experimental systems, the accumulation of oxygen radicals has been associated with the induction of cellular apoptosis, and some groups have recently described programmed cell death in *Leishmania* species and other unicellular organisms that results from oxidative stress (Duszenko et al., 2006; Kulkarni et al., 2009; Ye et al., 2009). Our observations pertaining to the rapid alterations in parasite morphology after a brief cultivation with $GR1^+$ monocytes would be consistent with an apoptotic mechanism of parasite death. The mechanisms by which $GR1^+$ monocytes induce parasite death will be the subject of further studies.

Platelets have been shown to be very important in hemeostasis and in the pathogenesis of cardiovascular disease. Now more attention is being given to their role in the pathogenesis of infectious diseases, including Malaria (Bruchhaus et al., 2007), Aspergillosis (McMorran et al., 2009), and bacterial infections (Yeaman 2010). This role is attributed to their capacity to release cytokines and chemokines, mediating inflammation and immune responses. In the present study, we demonstrate that platelets can be activated by *Leishmania* spp. to recruit an important subset of effector monocytes that can influence the outcome of disease. In this regard, platelets can be considered one of the first cells to initiate innate immune responses to this organism. Platelets are likely to be present in high numbers at the site of infection in the pool of blood created during the sandfly meal. The direct inhibition of platelet activation by sandfly saliva may be an important mechanism to limit effector monocyte recruitment during infection. Furthermore, the inhibition of complement activation by sandfly saliva may also decrease the migration of these monocytes into lesions. The contribution of activated platelets to innate host defense will most likely extend to many other infectious organisms that activate complement. We therefore anticipate that the studies presented in this work may extend to many infections in which activated platelets mobilize monocytes and contribute to host defense.

MATERIALS AND METHODS

Mice. These studies were reviewed and approved by the University of Maryland Institutional Animal Care and Use Committee (IACUC). BALB/c and C57BL/6 mice were purchased from the National Cancer Institute Charles River Laboratories. Knockout mice rendered genetically deficient in complement fragment C3 ($C3^{-/-}$) or C5 ($C5^{-/-}$), in the gp91 phagocyte oxidase ($phox^{-/-}$), and in the recombinase 2 enzyme ($RAG2^{-/-}$) and transgenic mice expressing enhanced cyan-fluorescent protein C57BL/6 ^{ECFP} and green fluorescent protein driven by the fractalkine receptor $CX3CR1^{GFP/GFP}$ mice were purchased from The Jackson Laboratory. $CX3CR1^{GFP/GFP}$ mice were backcrossed with WT C57BL/6 mice to obtain cells expressing both GFP and CX3CR1 molecules ($CX3CR1^{GFP/+}$)[3]. These mice were used for in vivo experiments. The $CX3CR1^{GFP/GFP}$ mice were crossed with $RAG2^{-/-}$ mice, as previously described (Geissmann et al., 2003), to obtain mice expressing high numbers of monocytes in their blood. In brief, $CX3CR1^{GFP/GFP}$ mice were crossed to $RAG2^{-/-}$. Those homozygous mice ($CX3CR1^{GFP/GFP}RAG2^{-/-}$) were crossed back to $RAG2^{-/-}$ to obtain a strain with high numbers of monocytes expressing GFP and a functional CX3CR1. These mice were used for in vitro experiments on purified monocytes.

Parasites. *L. major* and RFP-*L. major* (WHO MHOM/IL/80/Friedlin) were isolated from infected BALB/c mice and grown as previously described (Conrad et al., 2007) In brief, parasites were grown in medium containing equal parts Schneider's insect medium (Sigma-Aldrich) and M-199 (Invitrogen) supplemented with 20% FBS, 100 U/ml penicillin, 100 µg/ml streptomycin, and 2 mM glutamine. RFP-*L. major* were developed by one of the authors (A. Debrabant) as previously described (Kimblin et al., 2008). Transgenic parasites were grown in the presence of 50 µg/ml of Geneticin (G418; Sigma-Aldrich). Mice were injected in the left hind footpad with 2×10^6 *L. major*, and lesion size was determined by using a caliper to measure the thickness of the infected footpad and subtracting the thickness of the contralateral uninfected footpad as described previously (Rødland et al., 2010). RFP-*L. major* promastigotes were used for the peritoneal infection experiments. Metacyclic parasites were obtained as previously described (da Silva and Sacks, 1987) and used for all killing experiments. In brief, stationary phase parasites were washed three times with DPBS and resuspended in RPMI containing 50 µg/ml peanut agglutinin (Vector Laboratories Inc.) and incubated for 15 min at room temperature. Parasites were centrifuged at low speed (500 RPM) for 10 min. The supernatant was collected and diluted with DPBS. The mixture was centrifuged at 3,500 RPM for 15 min to pellet metacyclic promastigotes.

MEFs. MEF were prepared following the protocol from Theo Ross at the University of Michigan from mouse fetuses harvested between day 12.5 and 14.5 of gestation. Minced tissue pieces were incubated with 2 ml trypsin-EDTA (Invitrogen) at 37°C for 10 min. After centrifugation at 350 *g* for 10 min, the pellets were resuspended with DME containing 10% FBS and 2 mM glutamine supplemented with 100 U/ml of penicillin and 100 µg/ml of streptomycin. The fetal tissue was vigorously pipetted to obtain a single cell suspension that was then incubated at 37°C. After three to five passages, the cells were used for experimentation as indicated in the figure legends.

Platelet isolation and depletion. Platelets from WT mice or from transgenic mice expressing an enhanced cyan fluorescent protein were isolated as previously described (Johnson et al., 1998) with the following minor modifications. In brief, 500 µl of blood was collected by cardiac puncture into 100 µl of 3.8% sodium citrate. 400 µl of cation-free PBS was added and mixed gently with the platelets, which were then centrifuged at 90 *g* for 12 min. Supernatants were collected and centrifuged at 2,000 *g* for 3 min. The platelet pellet was suspended in cation-free PBS and the number of platelets was counted. To transiently deplete platelets from mice, we injected intraperitoneally 2 µg of

anti-CD41 (clone eBioMWReg30; eBioscience) diluted in 100 µl of PBS, 18-24 h before initiating experiments.

Isolation of monocytes from blood and from footpads. To obtain monocytes from blood, mice were bled from the orbital plexus, and blood was collected in 3-mL vacutainer tubes with EDTA (BD). Blood was gently mixed with an equal volume of HBSS containing EDTA (0.3 mM) and isolated by density gradient centrifugation using Histopaque 1083 (Sigma-Aldrich) at 920 *g* at room temperature. Interface cells were collected and cells washed with DMEM and resuspended in PBS. The red blood cells were lysed using Pharm Lyse (BD) washed and resuspended in either staining buffer or PBS, depending on the experiment.

To obtain monocytes from footpads, mice were infected with 2×10^6 *L. major* in 10 µl saline in both footpads for the prescribed time, after which the footpads were excised. The skin was cut with scissors and the exposed tissue was placed in a 24-well plate containing 1.2 µg/ml of Liberase RI (Roche). The tissue was incubated for 1 h at 37°C, at which time the footpads were forced through a 70-µm cell strainer (BD) and washed with PBS. The red blood cells were lysed using Pharm Lyse and washed, and the remaining cells were resuspended in staining buffer.

Flow cytometry. Freshly isolated peritoneal or peripheral blood leukocytes, or cells isolated from infected footpads, were stained with mAb specific for F4/80-PE and F4/80-PB (BioLegend), and CD11b-PE/Cy7, CD11b PE, RB6-8C5-Percp/Cy5.5 (Anti-GR1), and CD115 PE (BD). Cells were gated on forward and side scatter to exclude cell debris and dead cells, using an aqua fluorescent reactive dye (L34957; Invitrogen) or propidium iodide (P4170; Sigma-Aldrich). Data were collected using a FACSCanto II (BD) with Diva (BD) and analyzed with FlowJo (Tree Star) software. The $GR1^+$ and $GR1^-$ monocytes were sorted based on $CX3CR1^{GFP}$ expression from $CX3CR1^{GFP/+}RAG2^{-/-}$ mice or stained for F4/80 PB and RB6-8C5 Percp/Cy5.5 from $RAG2^{-/-}$ mice and sorted using FACSAria II (BD Cell Sorter System; BD). Platelets were stained with antibody to CD41-FITC and CD62P-PE (eBioscience).

Microscopy and immunofluorescence. Monocytes were isolated from the blood or the peritoneum and cytospun onto glass slides for analysis of GFP expression (Fig. 1). For *L. major* killing assays, sorted $GR1^+$ and $GR1^-$ monocytes were seeded on coverslips and infected with a 5:1 ratio of RFP *L. major* to monocytes for 1 or 3 h in the presence of C5-deficient nonimmune serum. After brief washing with PBS, cells were fixed in methanol at 4°C for 15 min and then washed with PBS. For some studies, including those performed on monocytes from $phox^{-/-}$ mice, parasites were added to monocytes at a 5:1 ratio and cultivated unwashed for 3 d. At that time, viable parasite numbers were quantitated by limiting dilution assay, as previously described (Miles et al., 2005). To stain parasites by immunofluorescence, 5% anti–*L. major* immune serum from BALB/c mice was added to the monolayers for 20 min, followed by FITC goat anti–mouse IgG (eBioscience) for 30 min. The nuclei were counterstained for 1 min with 5 µg/ml propidium iodide. Slides were examined using an inverted fluorescence microscope (Axio Observer Inverted Microscope; Carl Zeiss, Inc.). Acquired images were used to count the number of parasites per cells and the number of infected cells. For *Leishmania*–platelet interactions, the assays were performed on 24-well tissue culture plates. RFP-*L. major* were incubated with ECFP platelets in the presence or absence of nonimmune serum from either wild-type, $C3^{-/-}$, or $C5^{-/-}$ mice. The images were acquired from 1 to 30 min using the Axio Observer Inverted Microscope. The movies were created and the images and parasite tracking were analyzed using the ImageJ software (National Institutes of Health).

ELISA. ELISAs were performed to detect mouse growth factors (PDGF-BB) using Quantikine Mouse/Rat PDGF-BB immunoassay kit (R&D Systems) or CCL2 (MCP-1) using OptEIA ELISA sets (BD) according to the manufacturer's instructions. ELISAs were developed using BD OptEIA substrate reagents and stopped with 2N H_2SO_4. Absorbance was read at 450 nm against 595 nm using a 96-well microplate photometer (Multiskan Ascent; Thermo Fisher Scientific).

To measure CCL2 and PDGF-BB in infected footpads, the feet were removed and strained through a 70-µm cell strainer, and washed with 500 µl of PBS. Tissue homogenates were centrifuged, and the supernatant was collected for ELISA and expressed relative to total protein, which was determined by the Bradford assay.

ROS detection. To detect ROS production at the single cell level, the Image-iT LIVE Green Reactive Oxygen Species Detection kit (I36007; Invitrogen) was used following the manufacturer's instructions. In brief, monocytes were washed twice with HBSS and incubated with 1:10 ratio of metacyclic *L. major* for 30 min. Next, prewarmed H_2DCFDA was added to the cells for 30 min at 37°C. The cells were incubated with Hoechst for the last 5 min to stain the nuclei of the cells. The cells were immediately analyzed by fluorescence microscopy. To quantitate ROS production at the population level, monocytes and *L. major* were co-cultivated at 37°C in HBSS containing 25 µM H_2DCFDA. Measurements were made every 10 min by fluorometer for a total of 3 h.

Parasite burden quantitation. A qPCR method to amplify parasite DNA was used to quantify parasite burden (Yang et al., 2010). In brief, the infected footpads were collected at different times and treated with proteinase K (Sigma-Aldrich) at 56°C in the presence of 10 mM EDTA overnight. The DNA was obtained after phenol/chloroform extraction and NaOAC/EtOH precipitation. Primers specific for *L. major* 18S rRNA gene were as follows: 5′-ATCGGCATCATCAGCGGCGG-3′ (sense) and 5′-TCGACGGGTGGTGGCCAATGTGC-3′ (antisense). PCR amplification of murine 18S rRNA gene was used as reference marker for normalization. The primers used were as follows: 5′-CCCAGTAAGTGCGGGTCATA-3′ (sense) and 5′-AGTTCGACCGTCTTCTCAGC-3′ (antisense). qPCR was conducted with the LightCycler 480 sequence detection system (Roche) using iQ SYBR Green Supermix (Bio-Rad Laboratories) following the manufacturer's instructions. The parasite burden was expressed as fold changes by using the $\Delta\Delta C_T$ method, as previously described (Yang et al., 2007).

Online supplemental material. Fig. S1 shows ROS production by GR1+ monocytes. Fig. S2 shows the depletion of mouse platelets by intraperitoneal injection of α-CD41 antibody in vivo. Fig. S3 shows that CCL2 (MCP-1) production from MEFs was inhibited by blocking the PDGF receptor. Fig. S4 shows the recruitment of effector monocytes after *L. major* infection in the footpad after platelet depletion. In Video 1, $GR1^+$ monocytes from WT mice were incubated with metacyclic *L. major* promastigotes for 1 h. In Video 2, $GR1^-$ monocytes from WT mice were incubated with metacyclic *L. major* promastigotes for 1 h. In Video 3, $GR1^+$ monocytes from $Phox^{-/-}$ mice were incubated with *L. major* parasites. In video 4, $GR1^+$ monocytes from $Phox^{-/-}$ mice were co-cultured with metacyclic *L. major* promastigotes, and parasite movement was tracked. In video 5, the lack of platelet activation is shown after the incubation of platelets with *L. major* parasites in the presence of $C3^{-/-}$ serum (lacking active complement). In video 6, platelet activation in the presence of $C5^{-/-}$ serum containing opsonic complement and *L. major* parasites. Online supplemental material is a available at http://www.jem.org/cgi/content/full/jem.20101751/DC1.

This work was supported in part by National Institutes of Health grant AI49383.
The authors have no competing financial interests in this work.

Submitted: 20 August 2010
Accepted: 22 April 2011

REFERENCES

Afonso, L.C., and P. Scott. 1993. Immune responses associated with susceptibility of C57BL/10 mice to *Leishmania amazonensis*. *Infect. Immun.* 61:2952–2959.

Alberta, J.A., K.R. Auger, D. Batt, P. Iannarelli, G. Hwang, H.L. Elliott, R. Duke, T.M. Roberts, and C.D. Stiles. 1999. Platelet-derived growth factor stimulation of monocyte chemoattractant protein-1 gene expression is mediated by transient activation of the phosphoinositide 3-kinase signal transduction pathway. *J. Biol. Chem.* 274:31062–31067. doi:10.1074/jbc.274.43.31062

Andrae, J., R. Gallini, and C. Betsholtz. 2008. Role of platelet-derived growth factors in physiology and medicine. *Genes Dev.* 22:1276–1312. doi:10.1101/gad.1653708

Auffray, C., D. Fogg, M. Garfa, G. Elain, O. Join-Lambert, S. Kayal, S. Sarnacki, A. Cumano, G. Lauvau, and F. Geissmann. 2007. Monitoring of blood vessels and tissues by a population of monocytes with patrolling behavior. *Science.* 317:666–670. doi:10.1126/science.1142883

Auffray, C., M.H. Sieweke, and F. Geissmann. 2009. Blood monocytes: development, heterogeneity, and relationship with dendritic cells. *Annu. Rev. Immunol.* 27:669–692. doi:10.1146/annurev.immunol.021908.132557

Barbalat, R., L. Lau, R.M. Locksley, and G.M. Barton. 2009. Toll-like receptor 2 on inflammatory monocytes induces type I interferon in response to viral but not bacterial ligands. *Nat. Immunol.* 10:1200–1207. doi:10.1038/ni.1792

Beaulieu, L.M., and J.E. Freedman. 2010. The role of inflammation in regulating platelet production and function: Toll-like receptors in platelets and megakaryocytes. *Thromb. Res.* 125:205–209. doi:10.1016/j.thromres.2009.11.004

Bruchhaus, I., T. Roeder, A. Rennenberg, and V.T. Heussler. 2007. Protozoan parasites: programmed cell death as a mechanism of parasitism. *Trends Parasitol.* 23:376–383. doi:10.1016/j.pt.2007.06.004

Conrad, S.M., D. Strauss-Ayali, A.E. Field, M. Mack, and D.M. Mosser. 2007. *Leishmania*-derived murine monocyte chemoattractant protein 1 enhances the recruitment of a restrictive population of CC chemokine receptor 2-positive macrophages. *Infect. Immun.* 75:653–665. doi:10.1128/IAI.01314-06

da Silva, R., and D.L. Sacks. 1987. Metacyclogenesis is a major determinant of *Leishmania* promastigote virulence and attenuation. *Infect. Immun.* 55:2802–2806.

de la Motte, C., J. Nigro, A. Vasanji, H. Rho, S. Kessler, S. Bandyopadhyay, S. Danese, C. Fiocchi, and R. Stern. 2009. Platelet-derived hyaluronidase 2 cleaves hyaluronan into fragments that trigger monocyte-mediated production of proinflammatory cytokines. *Am. J. Pathol.* 174:2254–2264. doi:10.2353/ajpath.2009.080831

Deshmane, S.L., S. Kremlev, S. Amini, and B.E. Sawaya. 2009. Monocyte chemoattractant protein-1 (MCP-1): an overview. *J. Interferon Cytokine Res.* 29:313–326. doi:10.1089/jir.2008.0027

Domínguez, M., and A. Toraño. 2001. *Leishmania* immune adherence reaction in vertebrates. *Parasite Immunol.* 23:259–265. doi:10.1046/j.1365-3024.2001.00380.x

Dunay, I.R., R.A. Damatta, B. Fux, R. Presti, S. Greco, M. Colonna, and L.D. Sibley. 2008. Gr1(+) inflammatory monocytes are required for mucosal resistance to the pathogen Toxoplasma gondii. *Immunity.* 29:306–317. doi:10.1016/j.immuni.2008.05.019

Duszenko, M., K. Figarella, E.T. Macleod, and S.C. Welburn. 2006. Death of a trypanosome: a selfish altruism. *Trends Parasitol.* 22:536–542. doi:10.1016/j.pt.2006.08.010

Fox, J.E. 2001. Cytoskeletal proteins and platelet signaling. *Thromb. Haemost.* 86:198–213.

Fukuoka, Y., and T.E. Hugli. 1988. Demonstration of a specific C3a receptor on guinea pig platelets. *J. Immunol.* 140:3496–3501.

Geissmann, F., S. Jung, and D.R. Littman. 2003. Blood monocytes consist of two principal subsets with distinct migratory properties. *Immunity.* 19:71–82. doi:10.1016/S1074-7613(03)00174-2

Getts, D.R., R.L. Terry, M.T. Getts, M. Müller, S. Rana, B. Shrestha, J. Radford, N. Van Rooijen, I.L. Campbell, and N.J. King. 2008. Ly6c^{+} "inflammatory monocytes" are microglial precursors recruited in a pathogenic manner in West Nile virus encephalitis. *J. Exp. Med.* 205:2319–2337. doi:10.1084/jem.20080421

Henderson, R.B., J.A. Hobbs, M. Mathies, and N. Hogg. 2003. Rapid recruitment of inflammatory monocytes is independent of neutrophil migration. *Blood.* 102:328–335. doi:10.1182/blood-2002-10-3228

Johnson, E.N., L.F. Brass, and C.D. Funk. 1998. Increased platelet sensitivity to ADP in mice lacking platelet-type 12-lipoxygenase. *Proc. Natl. Acad. Sci. USA.* 95:3100–3105. doi:10.1073/pnas.95.6.3100

Jung, S., J. Aliberti, P. Graemmel, M.J. Sunshine, G.W. Kreutzberg, A. Sher, and D.R. Littman. 2000. Analysis of fractalkine receptor CX(3)CR1 function by targeted deletion and green fluorescent protein reporter gene insertion. *Mol. Cell. Biol.* 20:4106–4114. doi:10.1128/MCB.20.11.4106-4114.2000

Kimblin, N., N. Peters, A. Debrabant, N. Secundino, J. Egen, P. Lawyer, M.P. Fay, S. Kamhawi, and D. Sacks. 2008. Quantification of the infectious dose of *Leishmania major* transmitted to the skin by single sand flies. *Proc. Natl. Acad. Sci. USA.* 105:10125–10130. doi:10.1073/pnas.0802331105

Kulkarni, M.M., W.R. McMaster, W. Kamysz, and B.S. McGwire. 2009. Antimicrobial peptide-induced apoptotic death of *Leishmania* results from calcium-dependent, caspase-independent mitochondrial toxicity. *J. Biol. Chem.* 284:15496–15504. doi:10.1074/jbc.M809079200

León, B., M. López-Bravo, and C. Ardavín. 2007. Monocyte-derived dendritic cells formed at the infection site control the induction of protective T helper 1 responses against *Leishmania*. *Immunity.* 26:519–531. doi:10.1016/j.immuni.2007.01.017

McMorran, B.J., V.M. Marshall, C. de Graaf, K.E. Drysdale, M. Shabbar, G.K. Smyth, J.E. Corbin, W.S. Alexander, and S.J. Foote. 2009. Platelets kill intraerythrocytic malarial parasites and mediate survival to infection. *Science.* 323:797–800. doi:10.1126/science.1166296

Miles, S.A., S.M. Conrad, R.G. Alves, S.M. Jeronimo, and D.M. Mosser. 2005. A role for IgG immune complexes during infection with the intracellular pathogen *Leishmania*. *J. Exp. Med.* 201:747–754. doi:10.1084/jem.20041470

Mosser, D.M., and P.J. Edelson. 1987. The third component of complement (C3) is responsible for the intracellular survival of *Leishmania major*. *Nature.* 327:329–331. doi:10.1038/327329b0

Mosser, D.M., and J.P. Edwards. 2008. Exploring the full spectrum of macrophage activation. *Nat. Rev. Immunol.* 8:958–969. doi:10.1038/nri2448

Mosser, D.M., T.A. Springer, and M.S. Diamond. 1992. *Leishmania* promastigotes require opsonic complement to bind to the human leukocyte integrin Mac-1 (CD11b/CD18). *J. Cell Biol.* 116:511–520. doi:10.1083/jcb.116.2.511

Ng, L.G., A. Hsu, M.A. Mandell, B. Roediger, C. Hoeller, P. Mrass, A. Iparraguirre, L.L. Cavanagh, J.A. Triccas, S.M. Beverley, et al. 2008. Migratory dermal dendritic cells act as rapid sensors of protozoan parasites. *PLoS Pathog.* 4:e1000222. doi:10.1371/journal.ppat.1000222

Palframan, R.T., S. Jung, G. Cheng, W. Weninger, Y. Luo, M. Dorf, D.R. Littman, B.J. Rollins, H. Zweerink, A. Rot, and U.H. von Andrian. 2001. Inflammatory chemokine transport and presentation in HEV: a remote control mechanism for monocyte recruitment to lymph nodes in inflamed tissues. *J. Exp. Med.* 194:1361–1373. doi:10.1084/jem.194.9.1361

Passlick, B., D. Flieger, and H.W. Ziegler-Heitbrock. 1989. Identification and characterization of a novel monocyte subpopulation in human peripheral blood. *Blood.* 74:2527–2534.

Peters, N.C., J.G. Egen, N. Secundino, A. Debrabant, N. Kimblin, S. Kamhawi, P. Lawyer, M.P. Fay, R.N. Germain, and D. Sacks. 2008. In vivo imaging reveals an essential role for neutrophils in leishmaniasis transmitted by sand flies. *Science.* 321:970–974. doi:10.1126/science.1159194

Poon, M., W.C. Hsu, V.Y. Bogdanov, and M.B. Taubman. 1996. Secretion of monocyte chemotactic activity by cultured rat aortic smooth muscle cells in response to PDGF is due predominantly to the induction of JE/MCP-1. *Am. J. Pathol.* 149:307–317.

Rødland, E.K., T. Ueland, T.M. Pedersen, B. Halvorsen, F. Muller, P. Aukrust, and S.S. Frøland. 2010. Activation of platelets by *Aspergillus fumigatus* and potential role of platelets in the immunopathogenesis of Aspergillosis. *Infect. Immun.* 78:1269–1275. doi:10.1128/IAI.01091-09

Rollins, B.J., T. Yoshimura, E.J. Leonard, and J.S. Pober. 1990. Cytokine-activated human endothelial cells synthesize and secrete a monocyte chemoattractant, MCP-1/JE. *Am. J. Pathol.* 136:1229–1233.

Sato, N., S.K. Ahuja, M. Quinones, V. Kostecki, R.L. Reddick, P.C. Melby, W.A. Kuziel, and S.S. Ahuja. 2000. CC chemokine receptor (CCR)2 is required for Langerhans cell migration and localization of T helper cell type 1 (Th1)–inducing dendritic cells. Absence of CCR2 shifts the *Leishmania major*–resistant phenotype to a susceptible state dominated by Th2 cytokines, B cell outgrowth, and sustained neutrophilic inflammation. *J. Exp. Med.* 192:205–218. doi:10.1084/jem.192.2.205

Semple, J.W., and J. Freedman. 2010. Platelets and innate immunity. *Cell. Mol. Life Sci.* 67:499–511. doi:10.1007/s00018-009-0205-1

Serbina, N.V., T.P. Salazar-Mather, C.A. Biron, W.A. Kuziel, and E.G. Pamer. 2003. TNF/iNOS-producing dendritic cells mediate innate immune defense against bacterial infection. *Immunity.* 19:59–70. doi:10.1016/S1074-7613(03)00171-7

Smyth, S.S., R.P. McEver, A.S. Weyrich, C.N. Morrell, M.R. Hoffman, G.M. Arepally, P.A. French, H.L. Dauerman, and R.C. Becker; 2009 Platelet Colloquium Participants. 2009. Platelet functions beyond hemostasis. *J. Thromb. Haemost.* 7:1759–1766. doi:10.1111/j.1538-7836.2009.03586.x

Sponaas, A.M., A.P. Freitas do Rosario, C. Voisine, B. Mastelic, J. Thompson, S. Koernig, W. Jarra, L. Renia, M. Mauduit, A.J. Potocnik, and J. Langhorne. 2009. Migrating monocytes recruited to the spleen play an important role in control of blood stage malaria. *Blood.* 114:5522–5531. doi:10.1182/blood-2009-04-217489

Strauss-Ayali, D., S.M. Conrad, and D.M. Mosser. 2007. Monocyte subpopulations and their differentiation patterns during infection. *J. Leukoc. Biol.* 82:244–252. doi:10.1189/jlb.0307191

Strieter, R.M., R. Wiggins, S.H. Phan, B.L. Wharram, H.J. Showell, D.G. Remick, S.W. Chensue, and S.L. Kunkel. 1989. Monocyte chemotactic protein gene expression by cytokine-treated human fibroblasts and endothelial cells. *Biochem. Biophys. Res. Commun.* 162:694–700. doi:10.1016/0006-291X(89)92366-8

Tsou, C.L., W. Peters, Y. Si, S. Slaymaker, A.M. Aslanian, S.P. Weisberg, M. Mack, and I.F. Charo. 2007. Critical roles for CCR2 and MCP-3 in monocyte mobilization from bone marrow and recruitment to inflammatory sites. *J. Clin. Invest.* 117:902–909. doi:10.1172/JCI29919

van der Heyde, H.C., I. Gramaglia, G. Sun, and C. Woods. 2005. Platelet depletion by anti-CD41 (alphaIIb) mAb injection early but not late in the course of disease protects against Plasmodium berghei pathogenesis by altering the levels of pathogenic cytokines. *Blood.* 105:1956–1963. doi:10.1182/blood-2004-06-2206

van Gils, J.M., J.J. Zwaginga, and P.L. Hordijk. 2009. Molecular and functional interactions among monocytes, platelets, and endothelial cells and their relevance for cardiovascular diseases. *J. Leukoc. Biol.* 85:195–204. doi:10.1189/jlb.0708400

Villadangos, J.A. 2007. Hold on, the monocytes are coming! *Immunity.* 26:390–392. doi:10.1016/j.immuni.2007.04.006

von Hundelshausen, P., and C. Weber. 2007. Platelets as immune cells: bridging inflammation and cardiovascular disease. *Circ. Res.* 100:27–40. doi:10.1161/01.RES.0000252802.25497.b7

Yang, Z., D.M. Mosser, and X. Zhang. 2007. Activation of the MAPK, ERK, following *Leishmania amazonensis* infection of macrophages. *J. Immunol.* 178:1077–1085.

Yang, Z., X. Zhang, P.A. Darrah, and D.M. Mosser. 2010. The regulation of Th1 responses by the p38 MAPK. *J. Immunol.* 185:6205–6213. doi:10.4049/jimmunol.1000243

Ye, Z., E.J. Kerschen, D.A. Cohen, A.M. Kaplan, N. van Rooijen, and S.C. Straley. 2009. Gr1+ cells control growth of YopM-negative yersinia pestis during systemic plague. *Infect. Immun.* 77:3791–3806. doi:10.1128/IAI.00284-09

Yeaman, M.R. 2010. Platelets in defense against bacterial pathogens. *Cell. Mol. Life Sci.* 67:525–544. doi:10.1007/s00018-009-0210-4

Yoshimura, T., and E.J. Leonard. 1990. Secretion by human fibroblasts of monocyte chemoattractant protein-1, the product of gene JE. *J. Immunol.* 144:2377–2383.

Yoshimura, T., N. Yuhki, S.K. Moore, E. Appella, M.I. Lerman, and E.J. Leonard. 1989. Human monocyte chemoattractant protein-1 (MCP-1). Full-length cDNA cloning, expression in mitogen-stimulated blood mononuclear leukocytes, and sequence similarity to mouse competence gene JE. *FEBS Lett.* 244:487–493. doi:10.1016/0014-5793(89)80590-3

Zhang, G., J. Han, E.J. Welch, R.D. Ye, T.A. Voyno-Yasenetskaya, A.B. Malik, X. Du, and Z. Li. 2009. Lipopolysaccharide stimulates platelet secretion and potentiates platelet aggregation via TLR4/MyD88 and the cGMP-dependent protein kinase pathway. *J. Immunol.* 182:7997–8004. doi:10.4049/jimmunol.0802884

Ziegler-Heitbrock, H.W., B. Passlick, and D. Flieger. 1988. The monoclonal antimonocyte antibody My4 stains B lymphocytes and two distinct monocyte subsets in human peripheral blood. *Hybridoma.* 7:521–527. doi:10.1089/hyb.1988.7.521